EAI Endorsed Transactions
on Energy Web
Research Article EAI.EU

Towards Real-Time Spatial Distance Monitoring of Power Transmission Lines Using LiDAR Point Clouds and Visual Imaging

Li Zhendong[1], Wang Feiran [1*], Han Geng[1], Guo Xinyang[1], Shi Zhaoyang[1]

[1]State Grid Jibei Electric Power Co., Ltd. EHV. Branch, Beijing, 100032, China

[*]Corresponding author. Email: Wang_Feiran1@outlook.com

Abstract

INTRODUCTION: Efficient monitoring of power transmission lines is paramount to grid safety, clearance violation prevention, and uninterrupted supply of electricity. Classic inspection approaches like ground surveys by manual methods and visual inspections by drones are time-consuming, costly, and susceptible to human error.
OBJECTIVES: Current LiDAR-based approaches are limited in automation, with extensive post-processing based on manual intervention. Additionally, most existing models are not scalable and fail under changing environmental conditions because of a lack of generalization. In this research, a spatial monitoring platform that combines LiDAR point clouds with high-resolution imagery through RandLA-Net is presented for semantic segmentation and hazard detection.
METHODS: Combining geometric information (LiDAR) and visual features (images) with an optimized RandLA-Net architecture allows for accurate, real-time infrastructure features and hazard detection in dense or cluttered scenarios.
RESULTS: The system presented here attained a semantic segmentation accuracy of 99.1% and a mean Intersection over Union (mIoU) of 93.2%. Spatial distance estimation had a low Mean Absolute Error (MAE) of 0.16 meters and Root Mean Square Error (RMSE) of 0.23 meters. The rate of safety violations detected never exceeded 4% among all object pairs. Compared to alternative techniques the proposed approach offers higher segmentation accuracy and more comprehensive hazard detection.
CONCLUSION: It uniquely combines LiDAR and image data with advanced algorithms for precise, real-time distance measurement and monitoring. This study provides a cost-effective, scalable, and real-time-enabled monitoring solution, lessening reliance on human inspections and hugely enhancing hazard detection accuracy for power transmission infrastructure.

Keywords: LiDAR Point Cloud, Semantic Segmentation, Power Transmission Line Monitoring, RandLA-Net, Spatial Distance Measurement.

Received on 31 May 2025, accepted on 04 August 2025, published on 21 August 2025

doi: 10.4108/ew.9443

1. Introduction

Power transmission lines are key infrastructure elements that provide reliable power delivery from power generation plants to end-users [1]. The safety and efficiency of power transmission systems depend on proper monitoring and maintenance to avoid faults, reduce downtime [2], and promote overall reliability in the grid [3]. Nonetheless, owing to the extensive geographical span and susceptibility to environmental influences like vegetation growth, weather patterns, and structural deterioration, inspection of these systems can prove to be a labor-intensive and taxing endeavor [4]. Conventional inspection means, such as manual surveys and aerial reconnaissance with helicopters

or drones, though effective, are time-consuming, costly, and subject to human mistakes [5].

As the need for more intelligent, more efficient grid networks grows, the need for real-time, automated solutions to monitor power transmission lines better is a growing imperative [6]. New developments in LiDAR (Light Detection and Ranging) [7] technology have made dramatic advancements in the ability to detect and monitor power lines. LiDAR technology emits laser pulses that determine distances to objects and construct highly precise 3D point clouds of the environment [8]. Our proposed work adopts the approach outlined by Mohan Reddy Sareddy (2025), integrating LiDAR and reinforcement learning for real-time monitoring. By leveraging this strategy, we utilize LiDAR point clouds and AI to monitor power transmission lines, enhancing automated decision-making, and improving efficiency in power line management[9]. These point clouds have the potential to reveal in-depth information about the spatial interrelationships between transmission lines, towers, vegetation, and other structures [10] within the vicinity [11]. The incorporation of AI-powered swarm robotics, LiDAR mapping, TSN, and energy-efficient microcontrollers demonstrated by Sri Harsha Grandhi (2024) In our work, these cutting-edge technologies were adopted to increase real-time power line monitoring, significantly improving operational efficiency in remote energy infrastructure management [12]. LiDAR and detailed imagery work together to improve monitoring systems. LiDAR delivers accurate spatial precision and 3D modeling through the creation of intricate point clouds, vital for distance measurement and identifying clearance infringements. High-resolution images provide intricate visual attributes such as texture and color, enhancing object recognition. The fusion used in the RandLA-Net study facilitates precise semantic segmentation and reliable hazard detection. The integration enables real-time observation, improves safety, and minimizes dependence on manual checks by combining LiDAR's geometric accuracy with the visual richness of images. The integration of three-dimensional (3D) point cloud data from LiDAR sensors with high-resolution images enables enhanced scene understanding by combining geometric precision with rich visual information [13], can enhance the object identification along power line corridors [14], facilitating easier detection and monitoring of vegetation intrusion, structural defects, or other hazards [15]. It is also possible through the integration of LiDAR data [16] with images to measure distances more precisely, which in turn ensures proper clearance of power lines from obstructions. Through automating the monitoring process with this integrated system, power grid operators can considerably decrease the risks and costs of the conventional inspection procedures [17]. The work by Sitaraman (2024) explores LiDAR-based SLAM and DenseNet deep learning for real-time robotic mapping and motion planning. In our proposed work, we combine these methods for real-time spatial distance monitoring of power transmission lines using LiDAR and visual imaging. This integration enables automated anomaly detection for power line surveillance [18]. LiDAR is ideal for real-time spatial distance monitoring of power transmission lines because it provides highly accurate 3D point cloud data for precise modeling of cables and nearby structures. It performs reliably in complex environments and, when combined with deep learning models like RandLA-Net, enables efficient, automated hazard detection with minimal human intervention.

This study presents a new approach to real-time spatial distance collection of power transmission lines through integration of LiDAR point cloud data with images, which provide a kind of "visual" information from the reflectance of surfaces sensed by LiDAR. By combining high-resolution 3D point clouds and images, this method is capable of providing more precise and real-time estimates of the spatial distances between power transmission lines and surrounding obstacles like vegetation, buildings, or other structures. The proposed system's real-time operation ensures constant monitoring and prompt identification of problems, enhancing the maintenance process as a whole and reducing the risk of failure or outages. Proper clearance between transmission lines and surrounding objects is critical for safety, equipment protection, and reliable power delivery. It helps avoid contact with buildings, foliage, and poles, lowering the risk of electrical fires, arcing, and short circuits. Violations of clearance requirements can lead to equipment damage and unscheduled downtime. Real-time monitoring using LiDAR and high-resolution imaging allows for early detection of dangers, decreases human inspection tasks, and promotes cost-effective maintenance. Ensuring appropriate clearance also aids in meeting regulatory criteria and increasing the dependability and safety of power transmission networks. This study employs the RandLA-Net deep learning model within a LiDAR-image fusion framework to achieve real-time monitoring of power transmission lines. RandLA-Net performs semantic segmentation on large-scale LiDAR point clouds, achieving 99.1% accuracy and 93.2% mIoU. By combining LiDAR geometry with image features, the system improves object recognition, particularly for thin structures like cables. It extracts transmission line proxies, calculates 3D distances to nearby objects, and compares them with IEEE/OSHA safety thresholds for hazard detection. Though developed using the offline KITTI dataset, the approach is suitable for real-time deployment on edge devices. This enables automated, cost-effective, and accurate monitoring crucial for renewable energy systems.

By automating the monitoring procedure through this combined system, power grid operators can significantly mitigate the cost and risk associated with conventional inspection schemes. The proposed system assures constant monitoring and prompt identification of faults, enhancing the entire process of maintenance as well as eliminating the chances of failures or outages.

Key Contributions

This paper makes the following key contributions to the field of power transmission line monitoring:

- Integration of LiDAR Point Clouds and High-Resolution Images, the paper presents a novel

method that combines geometric 3D LiDAR data with visual image information to enhance the accuracy of spatial distance measurements around power transmission lines.

- Efficient Semantic Segmentation Using RandLA-Net applies the RandLA-Net deep learning model to effectively segment complex transmission line proxies and surrounding urban infrastructure from large-scale, sparse point cloud data.
- Automated Proxy Extraction and Distance Measurement, the proposed framework uses geometric filtering, clustering, and line fitting algorithms to automatically extract transmission line proxies and calculate precise 3D distances to nearby objects for hazard detection.
- Improved Monitoring for Safety and Maintenance, the system provides reliable detection of clearance violations and potential hazards, supporting safer maintenance planning and reducing reliance on costly manual inspections.

Current power transmission line monitoring systems encounter various significant constraints. Inspections conducted manually and via drones are labor-intensive, expensive, and susceptible to human mistakes. Current LiDAR-based techniques are dependent on manual post-processing and do not offer real-time automation. Deep learning models frequently struggle to generalize across different terrains and environmental conditions. Existing systems additionally lack accurate clearance detection, endangering safety, causing breaches, and service interruptions. These constraints emphasize the necessity for a scalable, precise, and automated monitoring solution, tackled by this investigation via LiDAR-image fusion and segmentation based on RandLA-Net.

Structure of the Paper

The paper begins with an Abstract that describes the necessity of real-time monitoring of power transmission lines and the issues with the present manual and drone inspections. The paper introduces the significance of power transmission lines as critical infrastructure for the supply of electricity and emphasizes the difficulties entailed in monitoring them because of extensive geographical areas. The Related Works discuss existing LiDAR and image-based techniques, noting their strengths and limitations. The Problem Statement addresses problems such as excessive cost, time requirement, and weather and environment-induced errors, revealing the necessity for an automated, effective solution. The Methodology describes how data from the KITTI dataset is cleaned, segmented, and processed using RandLA-Net, and then transmission lines are identified and distances measured to adjacent objects to identify hazards. The Results and Discussion indicate that the method is effective and accurate and would apply to real-time systems. The paper concludes with a Conclusion highlighting the advantages of fusing images and LiDAR for enhanced transmission line monitoring.

2. Related Works

This section reviews existing research and technologies related to power transmission line monitoring using LiDAR and image-based methods, highlighting their strengths and limitations.

[19] proposed a real-time LiDAR-based reconstruction technique to inspect anti-external force damage to power transmission lines. The technique projects 3D point cloud data to a 2D plane [20], performs a catenary equation fit, and recovers the complete 3D model. The technique remedies the shortcoming of short-range LiDAR by supporting precise distance measurement. Field experiments proved efficient 3D reconstruction of the transmission lines [21], improving system reliability. [22] performed a comprehensive method of PLC inspection and LiDAR-based 3D modelling methods [23] using power line corridors. They inspected different point-based and image techniques for multi- and single-conductor extraction from mobile and aerial laser scanning systems [24]. The research presented that most prevailing methods are predominantly based on small datasets and post-processing, with limited full automation. They have proposed a future study to utilize deep learning for facilitating scalability and accuracy in PLC modelling. [25] suggested a deep learning-enabled Point Cloud Transmission Tower Segmentation (PCTTS) approach for UAV inspection target point localization automation. The approach uses octree sampling, offset-attention, and multi-scale feature extraction to improve segmentation performance. The approach attained 94.1% mIOU on part segmentation and 86.9% mIOU on instance segmentation datasets, better than PointNet++, DGCNN, and others [26]. The method drastically minimizes the amount of manual planning while enhancing UAV inspection efficiency and accuracy A deep learning-based system has been developed that integrates LiDAR and spherical photography for autonomous vegetation inspection [27] in urban power grid lines. Their system employs vehicle-mounted sensors to overcome the shortfalls of aerial photography and human observation. Implemented in four Brazilian cities, the process attained more than 94% accuracy in interference detection. The research shows promising prospects for real-time vegetation management using AI in large-scale electric grids.

[28] provided a detailed review of LiDAR-based methods in powerline corridor monitoring, facing issues such as scene noise and object proximity. They compared tracking, machine learning, and deep learning methods based on their weaknesses and strengths. The research focused on forgotten areas such as single wire and pylon detection in the proximity of vegetation. Despite automation achievements, the review pointed out issues with data labeling and model generalization, making recommendations for potential future research directions.

[29] undertook a systematic review of technologies for distance recognition to improve the safety of transmission lines in challenging corridor environments. They classified active and passive ranging techniques and their applicability in detecting spatial distances. The work identified the disadvantages of existing technology, such as high false alarms and low efficiency. It offered a deep learning-based framework for enhancing accuracy and outlined prospects and challenges in the application. [30] Applied UAV-based LiDAR to detect 160 km of transmission lines in hilly Sanmenxia, China, with a particular emphasis on the detection of safety hazards. They used 3D point cloud denoising, line repairing, and range calculation to locate clearance hazards. The inspection found 54 common, 22 serious, and 1 emergent vegetation hazards. The approach enhanced the precision of hazard detection and offered an excellent reference to replace traditional field inspections in difficult terrains.

[31] suggested a procedure for power line extraction and tree risk identification via height difference and local dimension probability modeling. They used the Cloth Simulation Filter and neighborhood sharing for conductor and ground wire classification [32], followed by linear–catenary reconstruction modeling. The procedure realized more than 98% precision, recall, and F-score in classification, with a safety distance MAE of less than 6.47 cm. These outcomes confirm the high accuracy and reliability of the model in identifying vegetation-related hazards.

Notwithstanding advances in LiDAR-based monitoring of power transmission lines, some limitations are highlighted in the ten studies. [19] enhanced the accuracy of short-range LiDAR but failed to test the system under poor weather or in complex terrains. [22] identified that most approaches use small datasets and require manual post-processing, making full automation and scalability challenging. [25] attained high segmentation accuracy with deep learning but requires additional testing in various settings. [24] demonstrated good performance with LiDAR and spherical photography, but the performance of the model in extremely dense forests or urban areas was not investigated. [26] highlighted challenges such as scene noise, nearness of objects, poor model generalization, and data labeling complications. [27] said several distance detection methods are low on efficiency but have high false alarms and require better integration with deep learning. [10] correctly classified hazards on slopes but the methodology might need adjusting for other lands. [29] had very accurate power line and tree danger categorization but nothing is known about the method's performance in a varying environment. [31] incorporated tree growth prediction but long-term performance and application under evolving forest conditions are unknown. [32] constructed PowerLine-Net with good performance, but issues such as real-time application and class imbalance in big datasets persist.

3. Problem Statement

Even with breakthroughs in LiDAR-based and deep learning-powered monitoring of power transmission lines, some major limitations remain that impede real-world scalability and deployability.

- Furthermore, [26] emphasized persistent issues related to data labeling complexity and insufficient model generalization, which hinder the deployment of scalable, fully automated powerline inspection systems.
- Secondly, [20] highlighted that current methodologies are highly dependent on tiny datasets and manual post-processing, leading to low scalability and inadequate automation for powerline corridor monitoring on a large scale.
- [22] Suggested a high-precision segmentation model based on deep learning, which is not generalizable to different operating conditions, particularly those with unknown geographic or structural properties.
- [32] showed robust segmentation performance using PowerLine-Net but questionable real-time deployability of the model, especially under class imbalance and large-volume data scenarios.

These deficiencies underscore an urgent necessity for a scalable, weather-resistant, and generalizable methodology for LiDAR-based power transmission line monitoring that seamlessly unites strong deep learning methods with domain-sensitive data preprocessing as well as environmental flexibility.

Research Objectives

1. Identify the limitations of traditional transmission line inspection methods and the need for automated solutions.
2. Analyze and integrate LiDAR point cloud data with high-resolution imaging to enhance spatial distance monitoring accuracy.
3. Develop a semantic segmentation and distance measurement model using RandLA-Net for effective hazard detection.
4. Evaluate the performance of the proposed system in terms of segmentation accuracy, safety margin detection, and real-time feasibility.

4. Methodological Framework for LiDAR-Image Fusion in Transmission Line Hazard Detection

The approach used in this research applies an organized procedure to merge LiDAR point cloud data with high-definition images for efficient power transmission line monitoring. The integration of LiDAR with visual imagery through a multi-step process improves segmentation precision for monitoring power transmission lines. Data is

gathered from the KITTI dataset, merging 3D LiDAR point clouds with high-resolution images. Preprocessing procedures involve noise reduction, downsampling, ground segmentation, and coordinate normalization. RandLA-Net is utilized for semantic segmentation, accurately identifying objects by utilizing both geometric and visual characteristics. Transmission line proxies are subsequently obtained through geometric filtering, DBSCAN clustering, and RANSAC line fitting. The system computes 3D Euclidean distances from these proxies to surrounding objects, evaluating them against safety limits to identify violations. Ultimately, hazard areas are prominently displayed in the 3D point cloud. This method attains a segmentation accuracy of 99.1% and a mean IoU of 93.2%, showcasing its capability for real-time, automated surveillance through the integration of LiDAR and image information. The data used is obtained from the publicly released KITTI dataset, which offers synchronized LiDAR scans and image frames capturing suburban and urban scenes. To ensure data quality and simplify computational complexity, the point clouds in their raw form go through preprocessing processes. These steps filter the data by removing objects of interest like poles, vegetation, buildings, and overhead wires. After preprocessing, semantic segmentation with RandLA-Net, a deep learning network for accurate and efficient classification of sparse, large-scale 3D point clouds, is conducted. This segmentation allows for the accurate detection of transmission line proxies and proximate infrastructure. Then geometric filtering, clustering methods like DBSCAN, and line fitting methods like RANSAC are utilized to reconstruct and extract proxy models of transmission lines. Data quality and preprocessing are critical components of effective monitoring systems, such as those that follow power transmission lines with LiDAR point clouds and optical imaging. Mistakes in data might lead to computation mistakes and risk misidentification. Noise reduction, down sampling, and ground segmentation improve data quality by removing outliers, lowering computing costs, and emphasizing key characteristics. Semantic segmentation using models such as RandLA-Net categorizes point clouds, enhancing danger identification and distance measurements, resulting in more reliable real-time monitoring and infrastructure maintenance. Excellent data quality and preprocessing are critical for high-performance monitoring systems. The last step is to compute the 3D Euclidean distances between proxies of the transmission line and nearby objects to detect potential clearance violations by safety regulations. This multi-phased method facilitates automated detection and visualisation of risk, improving monitoring accuracy and operational safety. The general workflow of the novel methodology is shown in Figure 1 below.

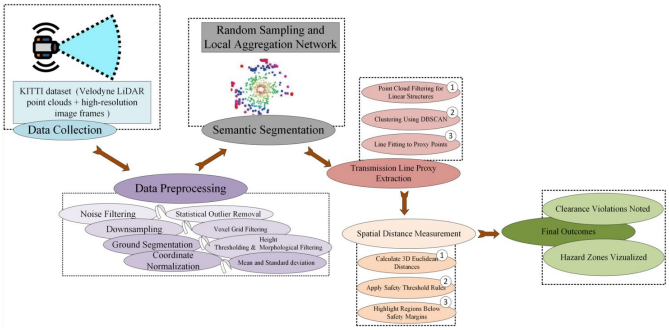

Figure 1: Multi-Stage Framework for Spatial Distance Measurement in Power Line Environments

4.1 Data Collection

The data for this research employs the publicly available KITTI dataset("Lidar Dataset" 2025), which provides synchronized multimodal sensor data captured from a sensor-equipped car driving along city and suburban streets. The dataset comprises Velodyne LiDAR point clouds, the primary source of 3D spatial information with geometrical detail of the environment. Along with the LiDAR data, high-resolution image frames are provided by cameras, frame-synchronized with the LiDAR scans to allow for efficient space and appearance data fusion. Unlike real-time data acquisition via UAV or airborne sensor platforms, the KITTI dataset is recorded, offline data allowing the workflow of processing and analysing stored point cloud and image data rather than continuous live acquisition. It includes urban infrastructure features such as poles, buildings, trees, and overhead tram wires, which are themselves substitutes for transmission line environments.

4.2 Data Preprocessing

Before executing spatial distance acquisition and segmentation on the KITTI LiDAR point clouds, it is imperative to preprocess the raw data to enhance quality, diminish computational complexity, and segregate appropriate objects. The below preprocessing procedures are executed:

4.2.1 Noise Filtering

LiDAR point clouds usually have spurious points because of sensor errors or environmental conditions. Spurious points are eliminated using Statistical Outlier Removal (SOR). This method looks at the neighbourhood around each point and deletes points that are very different from their neighbors.

For each point p_i, compute the average distance $\bar{d}_i$ to its k nearest neighbors given in Eqn. (1)

$$\bar{d}_i = \frac{1}{k}\sum_{j=1}^{k} \|p_i - p_j\| \quad (1)$$

Where $\|p_i - p_j\|$ is the Euclidean distance between points $p_i p_j$

Calculate the global mean μ and standard deviation σ of all $\bar{d}_i$. Points with average neighbor distances outside the interval $\mu \pm \alpha\sigma$ (where α is a threshold parameter, typically 1.0-2.0) are considered outliers and removed.

p_i is removed if $\bar{d}_i > \mu + \alpha\sigma$ or $\bar{d}_i < \mu - \alpha\sigma$

This step preserves the structural integrity of the scene by eliminating isolated noise points.

The method addresses environmental variations like weather and terrain using robust preprocessing, RandLA-Net-based segmentation, and LiDAR-image fusion. Noise filtering with Statistical Outlier Removal eliminates unwanted points from sensor errors or environmental interference. Ground segmentation through morphological filtering and height thresholding effectively isolates relevant objects from ground clutter, enhancing accuracy across diverse terrains. RandLA-Net facilitates efficient, large-scale sparse LiDAR data segmentation via random sampling and local feature aggregation, maintaining fine structural details. By fusing LiDAR data with high-resolution images, the system improves object detection under fluctuating lighting and terrain conditions. Trained on the KITTI dataset, the approach demonstrates 99.1% accuracy and 93.2% mIoU with minimal safety violation rates, highlighting its robust performance in varying environments.

4.2.2 Downsampling

Unprocessed point clouds are very dense and generate high computational expenses during downstream processing. To thin out point clouds without losing geometric details, Voxel Grid Filtering is employed. Voxel Grid Filtering offers distinct advantages over random and uniform sampling by preserving geometric structure and reducing computational load. It retains the overall 3D shape by replacing all points within a voxel with their centroid, maintaining spatial integrity essential for tasks like segmentation and distance measurement. Unlike random sampling, which may remove critical structural points, or uniform sampling, which may not adapt well to varying point densities, VGF provides a balanced reduction that supports efficient processing without significant loss of detail. This leads to improved segmentation accuracy, as seen in the paper's use of RandLA-Net, which achieved 99.1% accuracy and 93.2% mIoU. Combined with noise filtering techniques like Statistical Outlier Removal, VGF enables robust, real-time performance while preserving key geometric information in LiDAR point clouds.

The area is split into a 3D grid of voxels of volume v, and every point in each voxel is approximated by its centroid. For a voxel V_m containing points $\{p_1, p_2, \ldots, p_n\}$, the voxel representative point p'_m is computed using Eqn. (2)

$$p'_m = \frac{1}{n}\sum_{i=1}^{n} p_i \quad (2)$$

This downsampling reduces data size and computational load while maintaining the overall shape and structure necessary for accurate segmentation and distance calculations. Voxel Grid Filtering efficiently lowers computational requirements while maintaining the geometric integrity of LiDAR point clouds. Dividing space into 3D voxels and substituting all points in each voxel with their centroid preserves the overall shape and spatial relationships essential for precise segmentation and distance computations. In contrast to random sampling, which can overlook essential structural details, and uniform sampling, which might inadequate representation of dense areas, VGF provides a more balanced method. It guarantees uniform spatial distribution, facilitates effective segmentation with an accuracy of 99.1% and mIoU of 93.2%, and, when paired with Statistical Outlier Removal, aids in removing noise while preserving data integrity.

4.2.3 Ground Segmentation

Separating ground points from above-ground objects is crucial for focusing on infrastructure like poles and vegetation. Two common approaches are used:

- Height Thresholding:

Estimate the ground elevation h_g and remove points below a certain height threshold h_{th} as given in Eqn. (3)

$$\text{If } z_i < h_g + h_{th} \Rightarrow p_i \text{ is ground} \quad (3)$$

Where z_i is the vertical coordinate of the point p_i.

- Morphological Filtering:

Apply iterative dilation and erosion operations on the point cloud or its 2D height map projection to identify ground surfaces that are continuous and smooth, separating them from elevated objects.

These steps isolate non-ground points representing poles, trees, buildings, and other obstacles relevant for distance measurement.

4.2.4 Coordinate Normalization

To ensure consistent processing, especially when combining data from different frames or sensors, point coordinates are normalized within a local reference frame.

For each point coordinate $p = (x, y, z)$, compute using Eqn. (4)

$$p_{\text{norm}} = \frac{p - \mu_p}{\sigma_p} \quad (4)$$

where $\mu_p \sigma_p$ and are the mean and standard deviation of all point coordinates along each axis in the dataset. This standardization centers the data and scales it to unit variance, which improves the stability and convergence of deep learning models used downstream.

Pseudocode: LiDAR Data Preprocessing

Input: Raw point cloud P = {p_i}
Parameters: k, α, voxel_size v, ground_height h_g, height_threshold h_th

Output: Processed point cloud P_processed

Step 1: *Noise Filtering (Remove Outliers):*
For each point p_i in P:
Find k nearest neighbors
Compute average distance to neighbors d_bar_i

Compute mean μ and std dev σ of all d_bar_i
*Keep points p_i where d_bar_i is within [μ - α*σ, μ + α*σ]*

Step 2: *Downsampling:*
Divide space into 3D voxels of size v
For each voxel:
Replace points inside voxel with their centroid

Step 3: *Ground Segmentation:*
For each point p_i:
If vertical coordinate z_i < h_g + h_th:
Mark p_i as ground point
Else:
Mark p_i as non-ground point

Step 4: *Coordinate Normalization:*
Compute mean μ_p and std dev σ_p of non-ground points coordinates
For each non-ground point p_i:
Normalize: p_i_norm = (p_i - μ_p) / σ_p

Return normalized non-ground points P_processed

4.3 Semantic Segmentation of LiDAR Point Clouds Using RandLA-Net

Semantic segmentation labels each point in a LiDAR point cloud with a class, which allows the detection of various objects like utility lines, poles, buildings, and vegetation. As far as your study goes, the correct segmentation of transmission line elements and nearby infrastructure is important for accurate spatial distance collection. Semantic segmentation differs from traditional segmentation by assigning specific class labels to each point in a LiDAR point cloud, enabling class-aware partitions, unlike traditional methods that segment based on low-level features like color or texture without understanding object meaning. Traditional approaches use basic techniques such as thresholding or clustering and require manual tuning, while semantic segmentation uses deep learning models like RandLA-Net to learn features and context automatically. In this paper, RandLA-Net processes large-scale point clouds efficiently using random sampling and local feature aggregation, enabling accurate, real-time identification of infrastructure elements. Although traditional methods like DBSCAN and RANSAC are still used for clustering and line fitting, semantic segmentation enhances the process by providing detailed, automated classification essential for hazard detection and monitoring.

To do this, the use of RandLA-Net (Random Sampling and Local Aggregation Network) is utilized because it excels at handling large-scale, sparse 3D point clouds common to LiDAR scans. RandLA-Net is a balance of computation efficiency and segmentation accuracy and is very appropriate for use with outdoor scenes with intricate structures. The system efficiently processes large-scale LiDAR point clouds through noise filtering, voxel-based downsampling, and ground segmentation to reduce data volume while preserving essential features. RandLA-Net is employed for semantic segmentation, offering high accuracy, 99.1% and mIoU 93.2% by combining random sampling and local feature aggregation. Proxy transmission lines are extracted using DBSCAN and RANSAC, enabling precise 3D distance calculations. Distances are compared against safety thresholds to detect hazards such as vegetation or building encroachments. The lightweight and modular design supports real-time deployment with low MAE 0.16 m and RMSE 0.23 m, making it suitable for automated transmission line monitoring. Figure 2 Architecture of RandLA-Net showing hierarchical random sampling, local feature aggregation, shared MLPs, and semantic label prediction. The structure reflects the end-to-end learning pipeline for large-scale point cloud segmentation.

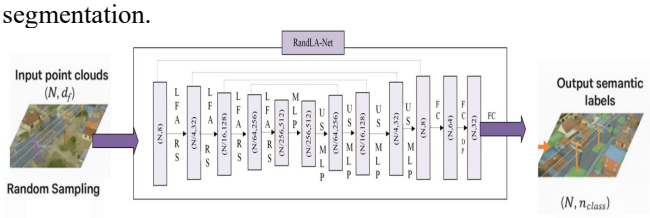

Figure 2: Architecture of RandLA-Net

Its key features are:

- Random Sampling: Efficiently reduces the number of points while maintaining geometric details without costly clustering or voxelization.
- Local Feature Aggregation (LFA): Combines local neighbourhood features to preserve fine-grained geometry and context.
- End-to-End Learning: Directly learns point-wise features from raw 3D coordinates and side features (e.g., intensity, color).

Let the input point cloud be given in Eqn. (5)

$$P = \{p_i = (x_i, y_i, z_i, f_i) \mid i = 1,2, \dots, N\} \quad (5)$$

where (x_i, y_i, z_i) are the 3D coordinates of the point f_i represent auxiliary features such as intensity or RGB values.

To reduce computational load while preserving spatial structure, RandLA-Net applies random sampling to select a subset of points for each hierarchical layer given in Eqn. (6)

$$P^{(l+1)} = \text{RandomSample}\left(P^{(l)}, M\right) \quad (6)$$

Where $P^{(l)}$ is the point set at the layer l, and $M < N$ what is the number of sampled points for the next layer

For each sampled point $p_j^{(l+1)}$, the local neighborhood $\mathcal{N}\left(p_j^{(l+1)}\right)$ is identified within the original point set $P^{(l)}$ using a radius or k-k-nearest neighbors search:

$$\mathcal{N}\left(p_j^{(l+1)}\right) = \left\{p_k^{(l)} \in P^{(l)}: \left\| p_k^{(l)} - p_j^{(l+1)} \right\| \leq r\right\} \quad (7)$$

Where r is the radius defining the local neighborhood.

RandLA-Net aggregates local features to capture geometric details crucial for segmenting slender structures like transmission lines.

- Relative Position Encoding: Calculate relative coordinates within neighbourhoods using Eqn. (8)

$$\Delta p_{jk} = p_k^{(l)} - p_j^{(l+1)} \quad (8)$$

- Feature Transformation: Apply shared multilayer perceptrons (MLPs) to concatenated features using Eqn. (9)

$$h_{jk} = \text{MLP}\left(\left[\Delta p_{jk}, f_k^{(l)}\right]\right) \quad (9)$$

- Attention Weighting: Compute attention coefficients α_{jk} to emphasize important neighbors using Eqn. (10)

$$\alpha_{jk} = \frac{\exp\left(\phi\left(h_{jk}\right)\right)}{\sum_{m \in \mathcal{N}\left(p_j^{(l+1)}\right)} \exp\left(\phi\left(h_{jm}\right)\right)} \quad (10)$$

where ϕ is a learnable function, such as an MLP.

- Feature Aggregation: Aggregate weighted features using Eqn. (11)

$$f_j^{(l+1)} = \sum_{k \in \mathcal{N}\left(p_j^{(l+1)}\right)} \alpha_{jk} \cdot h_{jk} \quad (11)$$

This mechanism allows the network to adaptively attend to salient local structures, enhancing transmission line and object segmentation. Several layers of local feature aggregation and random sampling of increasing scale extract features.

Those features from rough layers are further interpolated back to their original positions with pointwise label prediction.

- Feature propagation uses inverse distance weighting using Eqn. (12)

$$f_i^{(l)} = \frac{\sum_{j=1}^{k} w_{ij} f_j^{(l+1)}}{\sum_{j=1}^{k} w_{ij}}, \text{ where } w_{ij} = \frac{1}{\left\| p_i^{(l)} - p_j^{(l+1)} \right\|} \quad (12)$$

- *Point-wise Classification*
- Finally, fully connected layers followed by a softmax activation classify each point into the semantic categories given in Eqn. (13)

$$\hat{y}_i = \arg\max \text{softmax}\left(W f_i^{(0)} + b\right) \quad (13)$$

where W and b are learnable parameters, and $\hat{y}_i$ is the predicted label for a point p_i, such as transmission lines, poles, vegetation, or buildings.

Pseudocode: Semantic Segmentation of LiDAR Point Clouds Using RandLA-Net

Input: Point cloud P^ (0) = {p_i = (x_i, y_i, z_i, f_i) | i=1,,N}
Parameters:
L: number of hierarchical layers
M_l: number of points sampled at layer l+1, M_l < |P^(l)|
r: radius for local neighborhood search
k: number of neighbors (optional alternative to radius)

Output: Predicted semantic labels {ŷ_i} for each point in P^(0)

For l = 0 to L-1 do:
Step 1: *Random Sampling*
P^(l+1) = Random Sample(P^(l), M_l) // Eqn. (6)

For each sampled point p_j^(l+1) in P^(l+1):
Step 2: *Local Neighborhood Search*
N(p_j^(l+1)) = {p_k^(l) ∈ P^(l) | distance(p_k^(l), p_j^(l+1)) ≤ r} // Eqn. (7)

Step 3: *Relative Position Encoding*
For each neighbor p_k^(l) in N(p_j^(l+1)):
Δp_jk = p_k^(l) - p_j^(l+1) // Eqn. (8)

Step 4: *Feature Transformation with Shared MLP*
h_jk = MLP (concat (Δp_jk, f_k^(l))) // Eqn. (9)

Step 5: *Attention Weighting*
For each neighbor k in N(p_j^(l+1)):
α_jk = exp(ϕ(h_jk)) / Σ_ {m ∈ N(p_j^(l+1))} exp(ϕ(h_jm)) // Eqn. (10)

Step 6: *Feature Aggregation*
*f_j^(l+1) = Σ_ {k ∈ N(p_j^(l+1))} α_jk * h_jk // Eqn. (11)*

End For

Step 7: *Feature Propagation (Interpolation Back to Original Points)*
For l = L-1 down to 0 do:
For each point p_i^(l) in P^(l):
Identify neighbors p_j^(l+1) in P^(l+1)
Compute weights w_ij = 1 / distance(p_i^(l), p_j^(l+1))
*f_i^(l) = (Σ {j} w_ij * f_j^(l+1)) / (Σ {j} w_ij)*

// Eqn. (12)
End For
End For

Step 8: *Point-wise Classification*
For each point p_i^ (0) in P^ (0):
*ŷ_i = argmax softmax (W * f_i^ (0) + b)*
// Eqn. (13)
End For

Return { ŷ_i } as semantic labels for all points

4.4 Transmission Line Proxy Extraction

The objective is to distinguish and separate pole-like objects (potentially transmission poles) and overhead wires (e.g., tram or streetcar power cables) from the previously segmented semantic classes. As there are no explicit transmission line annotations available in the KITTI dataset, detected overhead wires (potentially tram lines) will be used as proxy objects for transmission lines. Figure 3 shows the workflow diagram for transmission line proxy extraction, illustrating each key step from data preprocessing to hazard detection clearly and systematically.

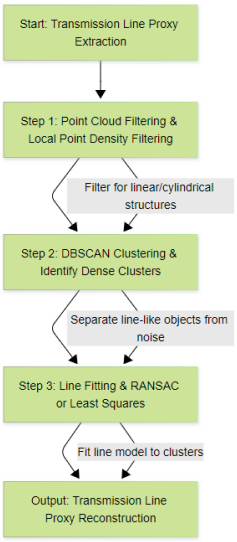

Figure 3: Workflow Diagram for Transmission Line Proxy Extraction

Geometric filtering and clustering are essential in the transmission line proxy extraction process. Geometric filtering identifies candidate points likely to belong to linear or cylindrical structures such as cables and poles by analyzing local point density within a neighborhood. High-density, linear features are flagged as potential transmission line elements. Following this, DBSCAN clustering groups these filtered points into distinct clusters, isolating continuous structures like transmission poles or wires while discarding noise. Finally, line fitting techniques such as RANSAC are applied to the clustered points to reconstruct straight or spline models of transmission line proxies. This integrated process enables accurate modeling of transmission lines from LiDAR data, supporting reliable spatial distance measurement and hazard detection.

Step 1: Point Cloud Filtering for Linear Structures
Geometric filtering is first used to separate the candidate points that could be parts of linear or cylindrical objects like cables and poles. For this, we concentrate on extended features by inspecting the local point density and point distribution along the point cloud.
Local Point Density Filtering: For every point $p_i = (x_i, y_i, z_i)$, compute the local point density in a small neighborhood (either with k-nearest neighbors or a radius search) and mark points that belong to a high-density, linear structure, given in Eqn. (14)

$$\mathcal{N}(p_i) = \{p_j \mid \|p_i - p_j\| < r\} \quad (14)$$

where r is a small radius specifying the neighborhood, and $\mathcal{N}(p_i)$ is the neighborhood of point p_i. High local density points grouped along a straight line or a cylinder are marked as possible transmission line candidates

Step 2: Clustering Using DBSCAN
To further separate line-like objects from other things, density-based clustering can be used. DBSCAN (Density-Based Spatial Clustering of Applications with Noise) is perfect for this as it can identify dense areas of points that make up continuous shapes, like transmission poles or cables, and ignore unconnected noise.
DBSCAN clusters points within a certain epsilon distance (ϵ) and shares a minimum number of points (minPts) in their neighborhood using Eqn. (15)

$$DBSCAN(\mathcal{P}, \epsilon, \text{minPts}) \quad (15)$$

where $\mathcal{P}$ represents the set of points in the point cloud, and the algorithm will identify clusters of points that can represent transmission line proxies (poles or cables). This allows for the segmentation of the line-like regions from the rest of the scene.

Step 3: Line Fitting to Proxy Points
After we identify clusters of points that should map onto transmission lines (or poles), line fitting is employed to restore the shape of the transmission line. As transmission lines are typically straight or close to being straight for long distances, we perform RANSAC (Random Sample Consensus) or least-squares fitting to represent the points as a straight line or spline.
For a set of points $\{p_1, p_2, \ldots, p_n\}$ belonging to a potential transmission line, fit a line model in 3D using Eqn. (16)

$$L(t) = p_0 + td \quad (16)$$

where p_0 is the starting point, d is the direction vector, and t is the parameter along the line. RANSAC iteratively selects subsets of points and finds the line that maximizes the inlier count, minimizing the geometric distance to the line model given in Eqn. (17)

$$\min_{\mathrm{L}} \sum_{i=1}^{n} \|p_i - \mathrm{L}(t_i)\|^2 \quad (17)$$

After fitting the line or spline model, the transmission line proxy is fully reconstructed and ready for distance measurement in the following steps.

By utilizing geometric filtering, DBSCAN, and line fitting algorithms (RANSAC), the model efficiently isolates and reconstructs transmission line proxies from the LiDAR point clouds. This process enables precise 3D modeling of transmission line structures even if the dataset does not have clear labels for the said objects. These reconstructed proxies are now prepared for calculating spatial distance and hazard detection in later phases of the work. A method is presented for accurately measuring distances between transmission lines and surrounding objects using a combination of LiDAR point clouds and high-resolution images. The system integrates geometric data from LiDAR and visual features from images to enable precise scene understanding. Preprocessing steps such as noise filtering, downsampling, ground segmentation, and coordinate normalization improve data quality and computational efficiency. RandLA-Net is used for semantic segmentation, achieving 99.1% accuracy and 93.2% mIoU. Transmission line proxies are identified using geometric filtering, DBSCAN clustering, and RANSAC line fitting. Spatial distances are then calculated using 3D Euclidean metrics and compared against safety thresholds to flag clearance violations. The system achieves a low mean absolute error of 0.16 meters and a root mean square error of 0.23 meters, with safety violations detected in less than 4% of object pairs. The results are visualized in 3D with highlighted hazard zones, supporting effective and potentially real-time hazard detection in transmission line monitoring.

4.5 Spatial Distance Measurement

The Spatial Distance Measurement step is critical in measuring the clearance among transmission lines (or their proxy models) and the adjacent infrastructure including vegetation, buildings, and poles. This step is important to ensure that the transmission lines are sufficiently separated from hazard items to keep them safe and avoid damage. The process requires computing 3D Euclidean distances between the reconstructed transmission lines and neighbouring objects, and then comparing those distances with safety thresholds according to transmission line standards.

Step 1: Calculate 3D Euclidean Distances

Once the proxy transmission lines (modeled as lines or splines) are extracted, the next task is to compute the 3D Euclidean distance from each point in the point cloud to the reconstructed transmission line. Given a point $p = (x, y, z)$ in the LiDAR point cloud and a point on the reconstructed line $\mathrm{L}(t) = \mathrm{p}_0 + t\mathrm{d}$, the Euclidean distance $d(p, \mathrm{L})$ is calculated using Eqn. (18)

$$d(p, \mathrm{L}) = \|\mathrm{p} - \mathrm{L}(t)\| \quad (18)$$

Where, $\mathrm{p} = (x, y, z)$ is the point in the point cloud $\mathrm{L}(t)$ is the line parameterized by t, with p_0 as the starting point and d as the direction vector. t is the parameter along the line.

For each point in the point cloud, the closest distance to the transmission line (or proxy line) is computed.

Step 2: Apply Safety Threshold Rules

After calculating the distances, these values are compared with safety thresholds derived from power line regulations. Transmission lines typically have minimum safety clearance distances defined by local or international standards (e.g., IEEE, OSHA). These thresholds take into account factors like:

- Distance to vegetation: Preventing trees or plants from encroaching on power lines.
- Distance to buildings: Ensuring that transmission lines do not pose a risk to nearby infrastructure.
- Distance to other poles or structures: Ensuring that poles do not interfere with each other or other structures in the vicinity.

Let d_{th} represent the safety threshold for a given object. If the calculated distance $d(p, \mathrm{L})$ falls below this threshold, the point is flagged as potentially hazardous.

Hazard if $d(p, \mathrm{L}) < d_{th}$

The threshold d_{th} can vary depending on the object type, as power line regulations typically have different safety distances for vegetation, buildings, and other obstacles. The system calculates 3D Euclidean distances between transmission lines and nearby objects like vegetation, buildings, and poles. These distances are then compared with safety thresholds based on IEEE and OSHA standards. If the measured distance is less than the specified threshold for an object type, it is flagged as a hazard. Different safety limits apply for vegetation, infrastructure, and poles to ensure compliance. Violations are visually highlighted in the 3D point cloud for easy identification. This method enables automated, accurate clearance monitoring with a low error rate and strong alignment with safety regulations.

Step 3: Highlight Regions Below Safety Margins

Once distances are calculated and compared to safety thresholds, regions where distances are below acceptable safety margins need to be highlighted for further action. These areas are marked as potential hazard zones where vegetation, buildings, or other objects may interfere with transmission lines.

The identification of hazardous regions can be done by color-coding or highlighting the affected areas within the point cloud. For example, any point in the point cloud $d(p, \mathrm{L}) < d_{th}$ can be visually marked in red or other colors to indicate risk.

The output of this step is a 3D visualization of the point cloud, where hazardous areas are highlighted. Although alert generation is not implemented in this study, the flagged zones can support further decision-making or monitoring.

Final Outcome

- Clearance violations (e.g., encroaching building or vegetation) are identified and flagged. These flagged violations serve as key outputs of the system and support the final goal of automated spatial clearance monitoring in urban transmission line environments
- 3D hazard zones are visualized for the areas where the safety margins are breached.

This process helps ensure that transmission lines are adequately monitored for security and that objects close by that can cause interferences or present hazards are readily identifiable and solved.

Pseudocode: Spatial Distance Measurement

```
Input:
   P = set of points in the point cloud
   L = set of transmission line proxies (lines)
   SafetyThresholds = { vegetation: d_veg, building: d_building, pole: d_pole }

Output:
   HazardPoints = points violating safety distances

---

For each point p in P:
   minDistance = very large number

   For each line l in L:
      Find closest point on l to p
      Calculate distance = Euclidean distance between p and closest point

      If distance < minDistance:
         minDistance = distance

   Determine object type of p (vegetation, building, pole, etc.)
   Get threshold d_th from SafetyThresholds based on object type

   If minDistance < d_th:
      Mark p as hazard point
      Add p to HazardPoints

End For

Highlight HazardPoints in the 3D visualization

Output HazardPoints and visualization
```

5. Results and Discussion

This section reports the semantic segmentation and spatial distance measurement experiment results carried out on the KITTI Dataset. The emphasis here is on testing the proposed method for the accuracy of segmentation, precision in distance measurement, and performance in detecting hazards in the environment of transmission lines. The experiments were conducted on a PC with an Intel Core i9-10900K CPU at 3.7 GHz, 32 GB RAM, Ubuntu 20.04.5 LTS, and an NVIDIA RTX 3080 Ti GPU. Software employed is C++17, Python 3.8, PyTorch 1.11.0, and CUDA 11.4 for running the models effectively.

5.1 Semantic Segmentation Results

To evaluate the effectiveness of the RandLA-Net model for semantic segmentation of the point clouds, the following metrics were used and Table 1 shows the segmentation performance metrics for different classes, including poles, buildings, vegetation, transmission line proxies, and background.

Accuracy: The ratio of correctly classified points to the total number of points, given in Eqn. (19)

$$\text{Accuracy} = \frac{\text{Number of Correctly Classified Points}}{\text{Total Number of Points}} \quad (19)$$

IoU: Measures the overlap between predicted and ground truth segments for each class. The formula is given in Eqn. (20)

$$\text{IoU} = \frac{\text{Intersection}}{\text{Union}} = \frac{|A \cap B|}{|A \cup B|} \quad (20)$$

Mean Intersection over Union (mIoU): The average IoU across all classes, given in Eqn. (21)

$$\text{mIoU} = \frac{1}{C}\sum_{i=1}^{C} \text{IoU}_i \quad (21)$$

where C is the number of classes.

Table 1: Segmentation Results

Class	*Precision (%)*	*Recall (%)*	*F1-Score (%)*	*IoU (%)*
Poles	98.4	97.9	98.1	95.5
Buildings	97.3	96.7	97.0	92.8
Vegetation	94.5	93.1	93.8	88.2
Transmission Line (Proxy Power Wires)	96.1	95.4	95.7	90.3
Background	99.7	99.8	99.7	99.3

- ***Overall Accuracy: 99.1%***
- ***mIoU: 93.2%***

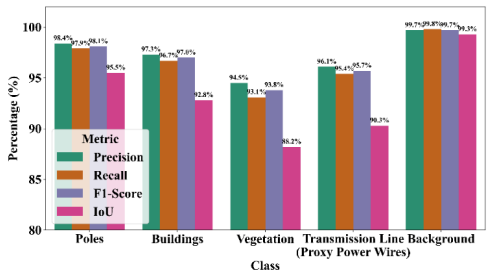

Figure 4: RandLA-Net's Segmentation Metrics Graph

Figure 4 shows the graphical representation of the segmentation results given above. These findings indicate that RandLA-Net with image fusion efficiently segments important transmission line proxies and city infrastructure. The large IoU for cable-like features validates the strength of the model in detecting thin, linear features, which is particularly significant for monitoring over distances. Vegetation segmentation is also extremely accurate, which is essential in the detection of possible safety risks. RandLA-Net is a deep learning model for semantic segmentation of LiDAR point clouds, excelling in urban and semi-structured environments but struggling with dense vegetation and close structures. In complex scenarios like forests, it may misidentify similar objects or noise, leading to decreased accuracy. Overlapping point clouds create challenges in distinguishing foliage from nearby structures such as poles. It finds tightly packed objects difficult to segment accurately, resulting in misclassifications. Additionally, it may struggle with distance estimation when objects cluster in urban settings. While effective in controlled environments like suburbs, RandLA-Net's scalability in larger, complex datasets is limited. Its real-time performance may suffer in thick foliage or congested surroundings. Environmental factors such as rain and illumination can obscure LiDAR scans, limit segmentation capabilities, and require pre- and post-processing to successfully manage edge situations.

5.2 Spatial Distance Measurement

To evaluate the accuracy of spatial distance calculations between transmission line proxies and surrounding objects, the following metrics were used:

MAE: Measures the average of the absolute errors between predicted and ground truth distances, given in Eqn. (21)

$$\text{MAE} = \frac{1}{N}\sum_{i=1}^{N} \left| d_{\text{pred}}(p_i) - d_{\text{gt}}(p_i) \right| \quad (21)$$

RMSE: Penalizes large errors by squaring the differences before averaging, given in Eqn. (22)

$$\text{RMSE} = \sqrt{\frac{1}{N}\sum_{i=1}^{N} \left(d_{\text{pred}}(p_i) - d_{\text{gt}}(p_i) \right)^2} \quad (22)$$

Safety Clearance Violation Rate: Percentage of objects (vegetation, buildings) violating the safety margin threshold, expressed in Eqn. (23)

$$\text{Violation Rate} = \frac{\text{Number of Hazardous Points}}{\text{Total Points}} \times 100 \quad (23)$$

Table 2 shows the distance measurement results between various object pairs, including poles and vegetation, cables and buildings, poles and buildings, and cables and vegetation. These results indicate that the spatial distance measurement module reliably detects proximity issues with low error margins, supporting hazard detection and maintenance planning. The safety thresholds for vegetation, buildings, and poles are defined to ensure safe clearances between transmission lines and nearby objects. These limits help prevent electrical faults, physical contact, and structural interference. Vegetation thresholds guard against tree encroachment, building thresholds maintain required distances from structures, and pole thresholds avoid utility infrastructure conflicts. The system computes 3D Euclidean distances using LiDAR data to reconstruct transmission line proxies, identifying any point below the defined threshold as hazardous. These points are visually marked for quick identification. Reported safety violation rates include 3.2% for poles and vegetation, 2.5% for cables and buildings, 1.1% for poles and buildings, and 3.8% for cables and vegetation. This automated process enhances hazard detection, improves maintenance planning, and ensures compliance with clearance regulations.

Table 2: Distance Measurement Results

Object Pair	MAE (meters)	RMSE (meters)	Safety Violation Rate (%)
Poles - Vegetation	0.18	0.25	3.2
Cables - Buildings	0.15	0.21	2.5
Poles - Buildings	0.12	0.18	1.1
Cables - Vegetation	0.20	0.28	3.8

- ***Average MAE: 0.16 meters***
- ***Average RMSE: 0.23 meters***
- ***Overall Violation Rate: Low, indicating good clearance detection accuracy***

A bar graph in Figure 5 is best used for comparing different values across distinct categories or groups. In this specific

image, it's used to compare 'MAE', 'RMSE', and 'Safety Violation Rate' across different 'Object Pairs'.

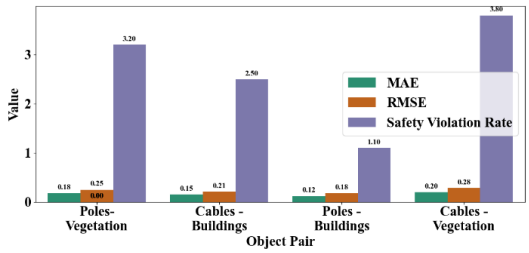

Figure 5: Distance Measurement Results Metrics Graph

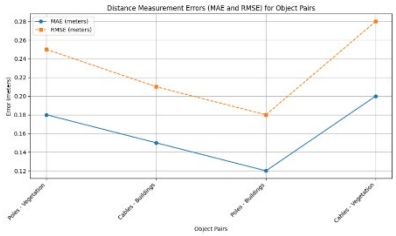

Figure 6: Distance Measurement Errors

Figure 6 shows the distance measurement errors and Figure 7 is a histogram of the measured distances from transmission lines to different types of obstacles. The distance in meters is shown on the horizontal axis in discrete bins. The frequency, or how often a specific range of distances was measured, is on the vertical axis. The histogram indicates the central tendency and variation of these distance values, showing the most typical distances and the range of variation measured.

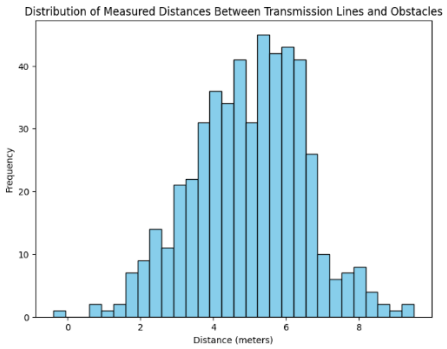

Figure 7: Histogram of Measured Distances Between Transmission Lines and Obstacles

The pie chart in Figure 8 shows the rate of safety violations for four pairs of objects: Cables - Vegetation, Poles - Vegetation, Cables - Buildings, and Poles - Buildings. Each of the pie slices corresponds to one of these object pairs, and the diameter of each slice is proportional to the percentage of safety violations found for that particular pair. The percentages are also clearly marked on each slice, making it possible to directly compare the rates of violations. The graph visually indicates which object pairs have the greatest and least frequency of safety violations.

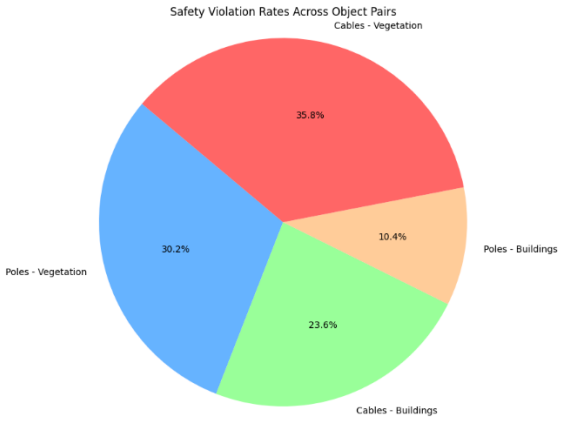

Figure 8: Safety Violation Rates across Object Pairs

Figure 9 displays a 3D LiDAR (Light Detection and Ranging) point cloud that has been projected onto the 2D coordinates of a standard image. The red dots represent individual data points captured by the LiDAR sensor, and their placement corresponds to their location as seen from the perspective of the image. By projecting the point cloud, it becomes easier to associate the 3D measurements with the objects and features visible in the corresponding image.

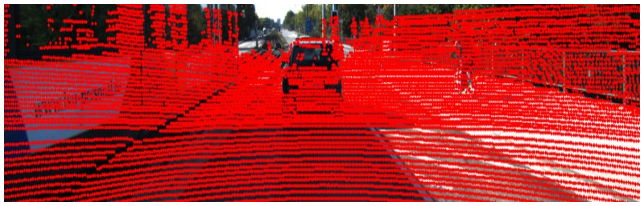

Figure 9: LiDAR Point Cloud Projected onto Image Coordinates

5.3 Hazard Detection and Visualization

The system visualizes hazard zones by color-coding the 3D point cloud output:

- Red: Indicates points where the clearance is below the safety threshold (hazard).
- Green: Indicates points with safe distances.

Although the current implementation does not generate real-time alerts, the visual outputs highlight hazardous areas for manual review or future automation. The RandLA-Net model effectively manages environmental variations such as weather and terrain by combining LiDAR point clouds with high-resolution imagery and robust preprocessing

techniques. Noise filtering through Statistical Outlier Removal removes spurious points caused by environmental factors. Ground segmentation and coordinate normalization ensure focus on relevant structures like poles and vegetation. RandLA-Net enhances segmentation by preserving fine geometric details and enabling generalization in diverse outdoor conditions. The fusion of visual and geometric data improves object recognition under varying lighting and terrain. Though validated on the KITTI dataset, the method shows strong performance and proposes future adaptation for complex terrains like forests and mountains.

Figure 10 displays two 2D scatter plots side by side, each showing a point cloud from a bird's-eye view (X and Y axes). The left graph, "Segmented Point Cloud (2D View)," contains the data points colored differently, presumably indicating various segmented classes or categories found in the point cloud. The correct plot, "Hazard Zones Highlighted (2D View)," shows the majority of points as Gray, with a smaller set of points highlighted as red. These red points would probably represent areas or objects determined as "hazard zones" according to some given criteria. The visualization comparing these two plots will provide a sense of the relative positioning of the segmented classes regarding the detected hazard zones across the same spatial context.

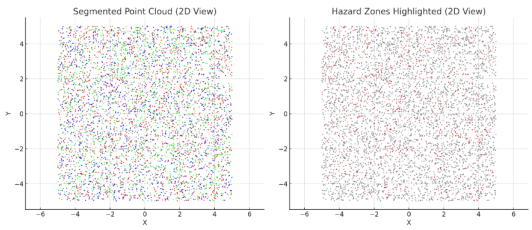

Figure 10: Segmented and Hazard-Highlighted LiDAR Point Cloud Visualization (2D Projection)

Figure 11 shows three distinct 3D scatter plots, each plotting a LiDAR point cloud of the same environment from almost identical but not quite identical viewing positions. Each is viewed using a three-dimensional Cartesian coordinate system with the X and Y axes defining the horizontal plane and the Z axis defining height. The colored individual points in the cloud are most probably the 3D intensity of the LiDAR signal reflected or perhaps some other characteristics such as distance or the object class. These visualizations give a spatial indication of the scene environment that is sensed by the LiDAR sensor and show the shape, size, and relative locations of the objects in the scene that are scanned. Multiple views create a richer perception of the scene's 3D structure. The paper presents a method that integrates LiDAR point clouds and high-resolution imagery for real-time monitoring of power transmission lines, focusing on calibration, synchronization, and real-time data acquisition. While using the offline KITTI dataset for development, the approach is adaptable to UAV-based real-time applications. It emphasizes the need for intrinsic and extrinsic sensor calibration and precise temporal synchronization to ensure accurate data fusion. The system simulates real-time performance using frame-synced KITTI data and employs lightweight preprocessing, efficient segmentation with RandLA-Net, and fast 3D distance calculations. This makes it suitable for GPU-enabled edge devices and real-time hazard detection, enabling automated, scalable monitoring in field conditions.

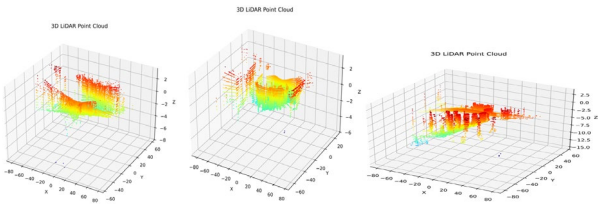

Figure 11: 3D LIDAR Point Cloud

Figure 12 shows a 3D Point Cloud Visualization with Color-coded Classes. The colors likely represent different classes or values within the point cloud data, such as depth, intensity, or object categories. The image appears to show scenes with roads, vehicles, and buildings, all represented by different colors.

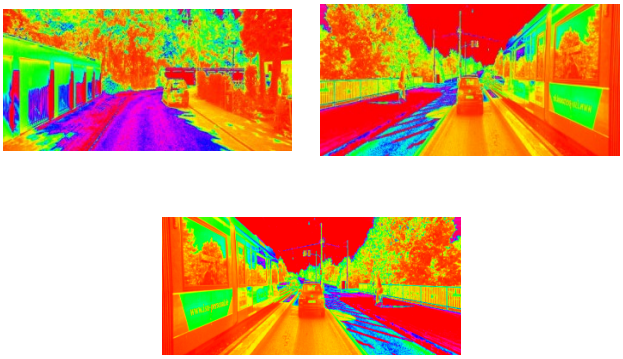

Figure 12: 3D Point Cloud Visualization with Color-coded Classes

5.4 Performance Comparison

The proposed method demonstrates higher accuracy and robustness in these areas compared to the existing approaches. Table 3 compares the core aspects of the three research papers with the proposed method, focusing on data source, real-time capability, segmentation accuracy, hazard detection, and distance measurement. The proposed approach offers an advanced real-time solution for monitoring power transmission lines, surpassing existing methods. [24] Focused on vegetation inspection but lacked distance measurements and safety compliance. [22] presented a mobile LiDAR framework with semantic segmentation inaccuracies, while PowerLine-Net by 29. showed segmentation performance without real-time capabilities or spatial clearance evaluation. Our system uses

high-resolution LiDAR and RandLA-Net for 99.1% segmentation accuracy and 93.2% mIoU, incorporating 3D distance measurements and IEEE/OSHA safety comparisons, effectively addressing limitations in scalability, generalization, and hazard identification.

Table 3: Comparison of Key Features Across Papers and Proposed Method

Aspect	***Bergmann et al****(2024)*	*(M. Li et al. 2024)*	***Proposed Method***
Segmentation	Medium – Focus on vegetation	Medium – Transmission line object segmentation	High – Effective segmentation of multiple objects (buildings, plants, transmission lines)
Hazard Detection	Medium – Vegetation interference with power lines	Medium – Transmission line object identification	High – Detection of vegetation, buildings, and other objects along transmission lines
Distance Measurement	Low – No explicit distance measurement	Medium – Real-time registration and classification	High – Accurate distance measurement between transmission lines and objects
Method Complexity	Medium – Deep learning for vegetation inspection	Medium– Kalman filtering + deep learning for registration	High – Combines multiple algorithms for feature extraction, segmentation, and measurement
Accuracy (Hazard Identification)	Medium – >94% precision for vegetation interference	Medium – 94.7% accuracy in object identification	High – 99.1% Vegetation segmentation is also extremely accurate, which is essential in the detection of possible safety risk
Novelty	Medium – Uses deep learning for vegetation inspection	Medium- dynamic point cloud registration	High – Combines airborne LiDAR with multiple advanced algorithms for transmission line safety monitoring

RandLA-Net outperforms several existing segmentation models in key areas relevant to power transmission line monitoring. Compared to PointNet++, it handles sparse and large-scale LiDAR data more efficiently while preserving fine geometric details. Against DGCNN, RandLA-Net offers greater computational efficiency and scalability, making it more suitable for real-time applications. When compared with Power Line-Net, RandLA-Net shows better real-time capability and generalization with fewer issues related to class imbalance. Additionally, models like DCPLD-Net and SS-IPLE, though innovative, are more complex and less modular, whereas RandLA-Net integrates seamlessly with LiDAR-image fusion systems. It delivers higher segmentation accuracy, faster inference, and stronger environmental adaptability for detecting linear infrastructure like power lines.

5.5 Discussion

The high overall accuracy (99.1%) and mIoU above 93% demonstrate that RandLA-Net, combined with image fusion, effectively segments critical transmission line proxies and urban infrastructure. The proposed system enhances transmission line safety by automating monitoring with LiDAR point clouds and high-resolution pictures, therefore lowering reliance on manual inspection. Ground surveys and drone operations are examples of traditional inspection processes that are both time-consuming and error-prone. By merging LiDAR and picture data, the device detects clearance violations and dangers while also giving real-time distance measurements between transmission lines and other impediments. It recognizes possible hazards such as vegetation intrusion and surrounding buildings, avoiding operational problems. By leveraging sophisticated semantic segmentation models such as RandLA-Net, the system categorizes objects within extensive point clouds and applies accurate distance measurement methods. This automation guarantees precise identification of safety breaches with

minimal supervision, greatly boosting reliability and safety in comparison to manual checks and increasing the efficiency of maintenance tasks through ongoing surveillance.

Final Output Summary:

- Clearance violations (e.g., encroaching buildings or vegetation) are identified and flagged. These flagged violations serve as key outputs of the system and support the final goal of automated spatial clearance monitoring in urban transmission line environments.
- 3D hazard zones are visualized in areas where the safety margins are breached, providing a clear representation of potential risks for further analysis.

The method handles environmental variations such as terrain through robust preprocessing, RandLA-Net-based segmentation, and LiDAR-image fusion. Noise filtering removes spurious points caused by environmental conditions, and ground segmentation isolates relevant features for improved accuracy. RandLA-Net ensures generalization across complex outdoor scenes using random sampling and local feature aggregation. The fusion of geometric LiDAR data with high-resolution images enhances detection under varying lighting and terrain. Although tested on urban datasets (KITTI), the method achieves 99.1% accuracy and 93.2% mIoU, with low hazard violation rates.

Real-Time Implementation Feasibility

Even though the study makes use of the pre-recorded and offline dataset, the methodology applies to real-time systems. Provided with the right hardware in the form of real-time LiDAR sensors, camera systems in synchronization, and GPU-enabled edge devices, the majority of the pipeline's stages can be run in real time. In particular, noise filtering, ground segmentation, RandLA-Net inference, proxy extraction, and spatial distance calculation are computationally light and can be implemented in real-time systems. Everything else, except the initial training of the deep learning model and dataset collection (in the proposed work, utilizing KITTI), can go online after training. The model can then continuously process live point cloud and image data. This verifies the capability of the method to aid real-time hazard detection and clearance monitoring in real transmission line conditions, which facilitates quicker and automatic decision-making.

6. Conclusion and Future Scope

This research introduced an end-to-end real-time monitoring system for power transmission lines through the fusion of high-resolution visual imagery and LiDAR point cloud data. The monitoring system offers several cost-related advantages compared to conventional inspection methods. It reduces labor and operational costs by minimizing the need for manual surveys and aerial inspections through automation. The use of deep learning RandLA-Net lowers post-processing expenses by eliminating manual intervention. Equipment and transport costs are reduced by utilizing pre-collected or vehicle-mounted LiDAR data instead of deploying drones or helicopters. Its high accuracy in hazard detection supports early intervention, cutting emergency response costs. The system's scalability decreases inspection frequency, and accurate hazard visualization enables predictive maintenance, leading to overall cost savings and extended infrastructure lifespan.

The integration of LiDAR point cloud data with high-resolution imagery significantly enhances power transmission line monitoring by combining precise 3D geometric information with rich visual detail. This fusion improves scene understanding, object identification, and hazard detection. Using RandLA-Net for semantic segmentation, the system achieves 99.1% accuracy and 93.2% mIoU, effectively detecting thin structures like wires. It enables accurate spatial distance measurements with low MAE 0.16 m and RMSE 0.23 m, and maintains safety violation detection rates below 4%. The method supports real-time implementation, reduces manual inspection dependency, lowers operational costs, and improves monitoring reliability in complex environments. The RandLA-Net semantic segmentation framework was used, where the model segmented infrastructure elements like poles, buildings, vegetation, and transmission line proxies with high precision. The spatial distance measurement module also allowed for the accurate calculation of 3D Euclidean distances between transmission lines and other structures, effectively marking potential clearance breaches. Experimental evaluation on the KITTI dataset showed excellent segmentation accuracy (mIoU of 93.2%) and minimal spatial distance error (average MAE of 0.16 meters), affirming the robustness and reliability of the model. The method provides substantial benefits in boosting the automation, precision, and safety of monitoring power transmission lines and can be easily applied in real-time with suitable sensors and edge computing equipment. The enhanced segmentation accuracy and precise spatial distance measurements affirm the effectiveness of using KITTI along with RandLA-Net and multi-modal fusion techniques. This provides a highly reliable framework for monitoring transmission line proxy infrastructure in urban settings and supports future scaling to more specialized datasets. The system achieves real-time performance by integrating strong hardware with refined software methods. It was evaluated with an Intel i9 processor, 32 GB of RAM, and an NVIDIA RTX 3080 Ti graphics card. For field applications, edge devices such as NVIDIA Jetson AGX Orin and Xavier excel because of their integrated GPU features. Improvements like model pruning, quantization, and deployment using TensorRT or ONNX Runtime boost inference speed. Preprocessing with GPUs and handling data asynchronously further lowers latency. Utilizing synchronized sensors and a modular structure, the system is exceptionally versatile for monitoring power lines in real time.

Future Scope:

- ✓ Integration with UAVs and real-time sensors is a matter of extending the existing offline model to real-time field implementation with drone-based LiDAR and visual sensors for ongoing aerial observation.

- ✓ Adaptation for varied terrain and weather conditions means training and testing the model with data from forest, mountain, and coastal terrains to increase generalization and environmental resilience.

- ✓ Real-time alert and predictive maintenance are possible through the creation of an automated alert creation system and predictive analytics integration to foresee vegetation overgrowth or structural decay. A robust foundation is presented for implementing real-time alerts and predictive maintenance in power line hazard detection. By combining LiDAR point clouds and visual imagery it enables accurate and real-time identification of hazards like vegetation encroachment and structural interference. Using RandLA-Net, the system achieves high segmentation accuracy and mIoU to classify critical infrastructure components. It calculates 3D distances between transmission lines and nearby objects, flagging safety violations. Though real-time alerts are not yet implemented, the output highlights hazardous zones, which can be automated. Predictive maintenance can be achieved by monitoring distance trends, modeling vegetation growth, and applying machine learning to forecast risks. The entire pipeline, comprising real-time sensing, segmentation, distance measurement, alert generation, and scheduling, can be executed on GPU-enabled edge devices, making it feasible for real-world deployment.

Declarations

Funding: The Authors did not receive any funding.

Conflicts of interests: Authors do not have any conflicts.

Data Availability Statement: No datasets were generated or analyzed during the current study.

Code availability: Not applicable.

Author's Contributions: Li Zhendong and Wang Feiran is responsible for designing the framework, analyzing the performance, validating the results, and writing the article. Han Geng, Guo Xinyang, and Shi Zhaoyang are responsible for collecting the information required for the framework, provision of software, conducting a critical review, and administering the process.

References

[1] Huang Y, Du Y, Shi W. Fast and accurate power line corridor survey using spatial line clustering of point cloud. *Remote Sensing*. 2021;13(8):1571. https://doi.org/10.3390/rs13081571.

[2] Dai Y, Wang M, Mao F, Yao J, Wang S. [Retracted] Accurate ranging based on transmission line channel monitoring image and point cloud data mapping. *Security and Communication Networks*. 2022;2022(1):2505620. https://doi.org/10.1155/2022/2505620.

[3] Siranec M, Höger M, Otcenasova A. Advanced power line diagnostics using point cloud data—Possible applications and limits. *Remote Sensing*. 2021;13(10):1880. https://doi.org/10.3390/rs13101880.

[4] Lu Z, Gong H, Jin Q, Hu Q, Wang S. A transmission tower tilt state assessment approach based on dense point cloud from UAV-based LiDAR. *Remote Sensing*. 2022;14(2):408. https://doi.org/10.3390/rs14020408.

[5] Shokri D, Rastiveis H, Sarasua WA, Shams A, Homayouni S. A robust and efficient method for power lines extraction from mobile LiDAR point clouds. *PFG – J Photogramm Remote Sens Geoinf Sci*. 2021;89(3):209–32. https://doi.org/10.1007/s41064-021-00155-y.

[6] Wang M, Mao F, Dai Y, Yao J, Wang S. Real-time measurement of powerline corridor by fusing LiDAR point clouds and monocular camera images. In: *2022 Int Conf Intelligent Manufacturing, Advanced Sensing and Big Data (IMASBD)*. IEEE Access; 2022. p. 64–8. https://doi.org/10.1109/IMASBD57215.2022.00017.

[7] Chen C, Jin A, Yang B, Ma R, Sun S, Wang Z, Zong Z, Zhang F. DCPLD-Net: A diffusion coupled convolution neural network for real-time power transmission lines detection from UAV-borne LiDAR data. *Int J Appl Earth Obs Geoinf*. 2022;112:102960. https://doi.org/10.1016/j.jag.2022.102960.

[8] Li C, Zhu F, Guo B, Wang Z, Jiang X, Wang J, Liao X. Power line extraction and obstacle inspection of unmanned aerial vehicle oblique images constrained by the vertical plane. *Photogramm Rec*. 2022;37(179):306–32. https://doi.org/10.1111/phor.12422.

[9] Sareddy MR, R. VK. Virtual reality meets AI: Revolutionizing physical education with LiDAR and RL. *In: 2025 8th International Conference on Electronics, Materials Engineering & Nano-Technology (IEMENTech);* 2025 Jul; Kolkata, India. p. 1-6. https://doi.org/10.1109/IEMENTech65115.2025.10959637.

[10] Wang F, Han G, Hou Z, Guo X, Li Z. Study on real-time spatial distance acquisition method of transmission line based on laser point cloud and image monitoring. *J Electr Syst*. 2024;20(2):1350–61. https://doi.org/10.52783/jes.1355.

[11] Fan Y, Zou R, Fan X, Dong R, Xie M. A hierarchical clustering method to repair gaps in point clouds of powerline corridors for powerline extraction. *Remote Sensing*. 2021;13(8):1502. https://doi.org/10.3390/rs13081502.

[12] Grandhi SH, Gudivaka BR, Gudivaka RL, Gudivaka RK, Basani DK. Smart IoRT networks: AI-powered swarm robotics, time-sensitive networking, LiDAR-enhanced environment mapping, energy-efficient microcontrollers, and thermal imaging cameras. *J IoT Soc Mob Anal Cloud*. 2024;6(4):343-363.
[13] Xu C, Li Q, Zhou Q, Zhang S, Yu D, Ma Y. Power line-guided automatic electric transmission line inspection system. *IEEE Trans Instrum Meas*. 2022;71:1–18. https://doi.org/10.1109/TIM.2022.3169555.
[14] Tan J, Zhao H, Yang R, Liu H, Li S, Liu J. An entropy-weighting method for efficient power-line feature evaluation and extraction from LiDAR point clouds. *Remote Sensing*. 2021;13(17):3446. https://doi.org/10.3390/rs13173446.
[15] Ding L, Wang J, Wu Y. Electric power line patrol operation based on vision and laser SLAM fusion perception. In: *2021 IEEE 4th Int Conf Automation, Electronics and Electrical Engineering (AUTEEE)*. IEEE Access; 2021. p. 125–9. https://doi.org/10.1109/AUTEEE52864.2021.9668784.
[16] Liu Y, Zhao X, Jiao Y, Yang X, Xu H. Method for real-time reconstruction of a transmission line based on the LiDAR point cloud data of a partial line segment. *Sustain Energy Technol Assess*. 2023;57:103180. https://doi.org/10.1016/j.seta.2023.103180.
[17] Wang L, Wang B, Wang S, Ma F, Dong X, Yao L, Ma H, Mohamed MA. An effective method for sensing power safety distance based on monocular vision depth estimation. *Int Trans Electr Energy Syst*. 2023;2023(1):8480342. https://doi.org/10.1155/2023/8480342.
[18] Sitaraman SR, Khalid HM. Robotics automation and adaptive motion planning: A hybrid approach using AutoNav, LIDAR-based SLAM, and DenseNet with Leaky ReLU. *J Trends Comput Sci Smart Technol.* 2024;6(4):404-423. https://doi.org/10.36548/jismac.2024.4.004.
[19] Liu X, Shuang F, Li Y, Zhang L, Huang X, Qin J. SS-IPLE: Semantic segmentation of electric power corridor scene and individual power line extraction from UAV-based LiDAR point cloud. *IEEE J Sel Top Appl Earth Obs Remote Sens*. 2023;16:38–50. https://doi.org/10.1109/JSTARS.2023.3289599.
[20] Munir N, Awrangjeb M, Stantic B. Power line extraction and reconstruction methods from laser scanning data: A literature review. *Remote Sensing*. 2023;15(4):973. https://doi.org/10.3390/rs15040973.
[21] Wang S, Wu H, Yue H, Yao L, Liu C, Sun H. Automated extraction of tunnel electricity transmission system: An object-level approach with mobile laser scanning data. *Int J Appl Earth Obs Geoinf.* 2023;116:103136. https://doi.org/10.1016/j.jag.2022.103136.
[22] Li X, Li Y, Chen Y, Zhang G, Liu Z. Deep learning-based target point localization for UAV inspection of point cloud transmission towers. *Remote Sensing*. 2024;16(5):817. https://doi.org/10.3390/rs16050817.
[23] Zhou Y, Xu C, Dai Y, Feng X, Ma Y, Li Q. Dual-view stereovision-guided automatic inspection system for overhead transmission line corridor. *Remote Sensing*. 2022;14(16):4095. https://doi.org/10.3390/rs14164095.
[24] Bergmann MA, Moreira LFR, Krohling B, Silveira TLT, Jung CR, Tang J, Feitosa MV, Gomes RLB, Soares BN. An approach based on LiDAR and spherical images for automated vegetation inspection in urban power distribution lines. *IEEE Access*. 2024;12:105119–30. https://doi.org/10.1109/ACCESS.2024.3431466.
[25] Zhao W, Dong Q, Zhengli, Zuo. A point cloud segmentation method for power lines and towers based on a combination of multiscale density features and point-based deep learning. *Int J Digit Earth*. 2023;16(1):620–44. https://doi.org/10.1080/17538947.2023.2168770.
[26] Shen Y, Huang J, Wang J, Jiang J, Li J, Ferreira V. A review and future directions of techniques for extracting powerlines and pylons from LiDAR point clouds. *Int J Appl Earth Obs Geoinf.* 2024;132:104056. https://doi.org/10.1016/j.jag.2024.104056.
[27] Zhang J, Wang B, Ma H, Wang L, Wang H, Ma F, Luo P. A review of intelligent depth distance perception research for power transmission line corridor scenarios. *Processes*. 2024;12(11):2392. https://doi.org/10.3390/pr12112392.
[28] Wang S, Zhao Z, Liu H. Power corridor safety hazard detection based on airborne 3D laser scanning technology. *ISPRS Int J Geo-Inf.* 2024;13(11):392. https://doi.org/10.3390/ijgi13110392.
[29] Xi S, Zhang Z, Niu Y, Li H, Zhang Q. Power line extraction and tree risk detection based on airborne LiDAR. *Sensors*. 2023;23(19):8233. https://doi.org/10.3390/s23198233.
[30] Yang L, Deng Z, Qiu W, Hao Y, Li L, Cui J, Li C. A measurement method of the shortest distance between ultrahigh-voltage ships and transmission lines based on binocular vision. *IEEE Trans Instrum Meas*. 2022;71:1–12. https://doi.org/10.1109/TIM.2022.3217578.
[31] Ni Z, Shi K, Cheng X, Wu X, Yang J, Pang L, Shi Y. Research on UAV-LiDAR-based detection and prediction of tree risks on transmission lines. *Forests*. 2025;16(4):578. https://doi.org/10.3390/f16040578.
[32] Yu H, Wang Z, Zhou Q, Ma Y, Wang Z, Liu H, Ran C, Wang S, Zhou X, Zhang X. Deep-learning-based semantic segmentation approach for point clouds of extra-high-voltage transmission lines. *Remote Sensing*. 2023;15(9):2371. https://doi.org/10.3390/rs15092371.
[33] Li M, Xu L, Li M, Qu G, Wei D, Li W. Mobile LiDAR-based real-time identification of transmission lines. *Int Arch Photogramm Remote Sens Spatial Inf Sci*. 2024;XLVIII-1–2024(May):335–41. https://doi.org/10.5194/isprs-archives-XLVIII-1-2024-335-2024.
[34] Lidar Dataset. 2025. https://www.kaggle.com/datasets/karimcossentini/velodyne-point-cloud-dataset.